

# Design of Lipid Emulsion-Dye Phantoms for Validation of Optical Imaging Systems

Amie Ha <sup>a,b</sup>, Ling Ma <sup>a,b</sup>, Mandy Yuan <sup>a,b</sup>, Izabella Chaverra <sup>a,b</sup>,  
Suhani Swain <sup>a,b</sup>, David R. Busch <sup>c</sup>, Baowei Fei <sup>a,b,d\*</sup>

<sup>a</sup> Center for Imaging and Surgical Innovation, University of Texas at Dallas, Richardson, TX

<sup>b</sup> Department of Bioengineering, University of Texas at Dallas, Richardson, TX

<sup>c</sup> Department of Anesthesiology & Pain Management, Neurology, Biomedical Engineering,  
UT Southwestern Medical Center, Dallas, TX

<sup>d</sup> Department of Radiology, UT Southwestern Medical Center, Dallas, TX

\*Corresponding author: [bfei@utdallas.edu](mailto:bfei@utdallas.edu), Website: <https://fei-lab.org>

## ABSTRACT

Optical phantoms are important for validation of optical imaging systems. The combination of polarized light imaging (PLI) and hyperspectral imaging (HSI) provides a novel tool to study biological and clinical questions. We previously developed a polarized hyperspectral imaging (PHSI) system for cancer detection. In this study, we developed multiple tissue-mimicking lipid emulsion-dye phantoms consisting of one of four dyes and lab-made lipid emulsion (LE) to measure the degree of polarization (DOP) through scattering of LE particles. The LE and dye components validate wavelength dependent changes in polarization within the imaging spectral range of 460 – 600 nm. Varying the LE concentration enabled controlled modulation of scattering strength, allowing systematic evaluation of polarization and reflectance responses. Results showed that these tissue-mimicking dye phantoms, at specific concentrations, produced reflectance and polarization trends that are relevant to the known absorption spectrum of the respective dye. Increased DOP was observed near each dye's absorption maximum, consistent with selective absorption of multiple scattered light. The lab-made lipid emulsion-dye phantom is tunable, has a low cost compared to commercial Intralipid, and can provide a more accessible approach to validating various optical imaging systems.

**Keywords:** Lipid emulsion-dye phantom, polarized hyperspectral imaging (PHSI), reflectance, scattering, polarization, validation

## 1. INTRODUCTION

Polarized hyperspectral imaging (PHSI) is an emerging optical imaging technique that acquires images over a broad range of wavelengths and utilizes polarized light to detect variations in tissue composition and structure. Prior studies have analyzed differences in tissue composition and microstructure of various skin abnormalities and scars [1, 2], tissue characteristics [3], as well as histological analysis of head and neck squamous cell carcinoma [4-6] and leukemia [7]. In our previous work, we developed a handheld PHSI system capable of full Stokes imaging [8]. To validate the probe's ability to detect different scattering levels, phantoms were made with varying concentrations of Intralipid and methylene blue as a scattering and absorbing agent, respectively. Tissue-mimicking phantoms are needed to assist in imaging techniques such as PHSI to validate if a PHSI probe can detect desired changes. However, PHSI is different from standard polarized imaging in that it is wavelength dependent, so it is important to validate the system across a wide spectral range. Moreover, various factors can impact the scattering, absorption, quality, and spectral signatures of the phantoms. Many works have cited the use of lipid emulsions (LEs), such as Intralipid, as a validation tool for optical imaging equipment and evaluated several factors affecting the stability of LE phantoms, including temperature and time. However, these studies often use commercial Intralipid and typically do not specify age of the emulsion, both of which may lead to optical properties which differ from a freshly made LE solution [9,10,13].

Intralipid is a highly scattering LE made from the suspension of glycerin, soybean oil, and an emulsifying agent in water [14]. It is commonly used as a scattering agent in the preparation of optical phantoms [9, 13]. However, to match tissue scattering properties, Intralipid must be diluted, a process that can lead to less precise scattering measurements at

the target concentration. Meanwhile, absorbers such as India ink, molecular probes, and tissue staining dyes can be utilized to make realistic, tissue-mimicking optical phantoms by varying their absorption properties. The ability to change the phantoms' spectral signature using different color dyes means that they can also be utilized to validate polarized hyperspectral imaging systems at different wavelengths.

In our current work, we developed tissue-mimicking phantoms using lab-made LE solutions and four different dyes to evaluate scattering spectra within the range of 460 – 600 nm. The goal of this paper is to develop and use these phantoms to validate the spectral performance of our PHSI system through analysis of LE concentrations, absorbing mediums, dye concentrations, and external factors affecting phantom stability. Using fresh, lab-made LEs in optical validation experiments is cost-effective and permits creation of experimental-specific concentrations of LEs.

## 2. METHODS

### 2.1 Lipid emulsion preparation and concentrations

Intralipid is commercially available at 20% and 30% (0.2 and 0.3 g lipid per ml) concentrations. Clinically, Intralipid provides intravenous nutrition to patients who cannot receive nutrition orally. In each 100 mL of commercial 20% Intralipid, there is 20 g soybean oil, 1.2 g phospholipids from powdered egg yolk, 2.25 g glycerin, water, and sodium hydroxide to adjust the pH. Although Intralipid is widely used as a tissue-mimicking scattering standard, its clinical-grade sourcing can make routine phantom validation costly and dependent on medical-supply access. Comparable lipid emulsions exhibit similar optical scattering behavior, but their availability is region dependent. Moreover, 10% is the lowest commercial Intralipid concentration, which has a much higher scattering coefficients than most tissues and does not show significant differences in DOP. Thus, optical phantoms typically use a few percent of stock Intralipid by volume.

In this work, we propose a lab-made LE recipe. Our lab-made LE consists of DI water, 2.25% v/v glycerin, 1.65% v/v polysorbate 80, and varying volumes of soybean oil depending on the target LE concentration. Egg phospholipids play an important role as emulsifiers to stabilize the solution, but they are difficult and expensive to obtain. Substitutes for egg phospholipids include casein and polysorbate 80, which are both relatively inexpensive [16], but we decided to use the latter because it allowed us to achieve a more stable emulsion compared to when we used the casein, where we observed oil phase separation. Lacking the literature developed for Intralipid optical phantoms, we needed to isolate the concentration range in our lab-made LE to where we could visualize the largest difference in DOP in the phantom. Once the ideal LE solution was identified, we could then proceed with adding dyes to the phantom to vary absorption.

To determine the target LE concentration, LE concentrations were created from 0% – 10% by diluting a 10% v/v stock. This stock was made by combining 2.625 mL glycerin, 1.125 mL polysorbate 80, and 7.50 mL soybean oil with 63.75 mL DI water to make a 75.00 mL solution. An ultrasonic homogenizer was used to emulsify the solution. To avoid phase separation in the final LE, we added 4.00 mL of soybean oil and emulsified first before adding the remaining 3.50 mL and emulsifying again. The prepared 10% LE stock was subsequently diluted with DI water to obtain various concentrations of LE. To make the 2.0% w/v agar for the phantom, we combined 3.00 mL glycerol and 4.00 g agar with 193 mL DI water, which we heated then cooled to 70°C (to prevent the emulsion from becoming unstable) before adding the LE solution. Then, 6.00 mL of each LE concentration was pipetted into a three-by-two well plate, along with 4.00 mL of agar to achieve a total volume of 10.00 mL per well. We made two phantoms of the same volume and size for each concentration to minimize variation and inconsistency. The resulting phantoms were 3.5 cm wide and 1 cm thick and were placed in a 2° – 8°C refrigerator to cool before being imaged.

After making and testing various LE concentrations from 0% – 10%, as shown in Figure 1, a concentration of 0.1% was found to effectively balance the signal intensity with polarization preservation, determined by identifying the concentration range with higher polarization values. Thus, the recipe of 1% v/v soybean oil, 2.25% v/v glycerin, 1.65% v/v polysorbate 80, and DI water was utilized to create a 1% solution that was then diluted with subsequent water or dyes to 0.1%. Finally, to validate our LE phantom, we measured its reflectance using a spectrometer to analyze its scattering properties.



|     |     |       |       |       |       |
|-----|-----|-------|-------|-------|-------|
| 10  | 10  | 1.25  | 1.25  | 0.156 | 0.156 |
| 5   | 5   | 0.625 | 0.625 | 0.078 | 0.078 |
| 2.5 | 2.5 | 0.313 | 0.313 | 0     | 0     |

**Figure 1.** The figure on the left shows the LE phantoms at different concentrations (0% – 10%). The table on the right indicates the specific concentrations for each set of phantoms, with there being two phantoms for each concentration. As the concentration increases, so does the reflectance of the phantoms, thus showing a higher brightness. The 0% phantoms contain no LE, only DI water to obtain a baseline for the scattering properties of the LE.

## 2.2 Absorbing mediums

When deciding the types of absorbing media to incorporate into our phantom, we needed to identify common and inexpensive water-soluble agents that fit in our spectral range of 460 – 600 nm. An additional factor we considered was whether the agent was a pigment or a dye since both differ in their solubility, light interactions, appearances, and scattering effects. Pigments are generally less water soluble, lighter in color, more stable over time, and exhibit Mie scattering due to their larger particle size. Dyes are generally more soluble, produce a more saturated color, fade over time, and exhibit Raleigh scattering due to their smaller particle size. As a result, the scattering properties of pigments and dyes will differ, since larger particle sizes can increase scattering and decrease DOP. To explore this difference, we compared methylene blue (MB) dye with two pigments, blue food colorant (FC, Goodman’s Food Coloring Kit, USA) and blue tissue staining (TS, IMEB, San Marcos, CA, USA) pigment, from our lab.

## 2.3 Absorber concentrations

Based on Beer’s law, absorption of light is directly proportional to concentration. in a sample. In the phantoms, the dyes act as absorbers to mimic how the imaging probe can detect various chromophores that may be present in human tissues. Scattering of light is reflected in the polarization values of the data. At a given scattering, the photon transport length will be lower at higher absorptions; thus, we anticipate the least depolarization (lowest number of scattering events) in detected photons at the peak of dye absorption. As such, there would be higher polarizations at the corresponding maximum absorption wavelengths, indicating less scattering. Methylene blue ( $\lambda_{\text{max}} = 665 \text{ nm}$ ), crystal violet ( $\lambda_{\text{max}} = 590 \text{ nm}$ ), tartrazine ( $\lambda_{\text{max}} = 425 \text{ nm}$ ), and safranin ( $\lambda_{\text{max}} = 520 \text{ nm}$ ) were the four dyes incorporated into the LE phantoms and evaluated. To assess the effect of concentration on the polarization and reflectance of the phantoms, we tested concentrations in % v/v, each prepared directly without dilution, of tartrazine ranging from 0.00025% – 0.09%, methylene blue from 0.00013% – 0.0005%, and safranin and crystal violet from 0.05% – 0.2%. Visual assessment was done to assess the similarity of DOP spectra trends to maximum absorbance spectra trends for each dye.

## 2.4 External factor considerations

With agar and water utilized for the phantoms, it is important to acknowledge that hydrogel phantoms have a more limited shelf life than other materials commonly utilized to create phantoms such as silicon and 3D printing materials. Factors including refrigeration time, phantom texture, hydration, and physical stability over time were considered and observed. Furthermore, the surface color on which the phantoms were imaged were explored due to the difference in absorbing and reflecting properties of white compared to black materials.

## 2.5 Validation

Validation of the handheld PHSI system in detecting various chromophores and scattering was conducted on these phantoms. Once the phantoms were prepared, they were taken out of the well plates, placed on a black imaging surface, and the back of the phantoms were imaged, primarily due to the presence of fewer artifacts such as air bubbles to avoid

introducing unwanted glare into the image and data analysis. Our handheld probe measured  $I_H$ ,  $I_V$ ,  $I_{45}$ , and  $I_{RC}$ , corresponding to horizontal, vertical, 45°, and right-circular polarized reflectance measurements, respectively, that allow for reconstruction of the Stokes parameters and polarization metrics such as degree of polarization (DOP), degree of linear polarization (DOLP), and degree of circular polarization (DOCP), as shown by Equations (1-2). Intensity image acquisition took less than a second for each phantom using in-house software, and the reflectance and polarization measurements were calculated in MATLAB (MathWorks, Natick, MA, USA) by selecting a 100×270 pixel region near the center of the phantom, which displayed the smoothest surface with least bubbles and glare. Measurements from the two samples were averaged since the values of their reflectance measurements were similar. Because the droplets in LEs are highly scattering, increasing the lipid concentration leads to higher scattering and, consequently, higher reflectance.  $I_{45}$  was also lower than  $I_H$  and  $I_V$ , which is consistent with our imaging system set-up. Because the handheld probe incorporates a fixed linear polarizer oriented at 45° on the illumination path, the incident light is already linearly polarized on the diagonal basis. As a result,  $I_{45}$  is inherently lower than  $I_H$  and  $I_V$ . This occurs because the 45° polarization state experiences greater attenuation at the tissue-air interface due to the polarization dependence of Fresnel reflectance, which preferentially reduces the p-polarized component of the diagonal state.

$$\begin{aligned}
 S_0 &= I_h + I_v \\
 S_1 &= I_h - I_v \\
 S_2 &= 2 \times I_{45} - S_0 \\
 S_3 &= 2 \times I_{rc} - S_0
 \end{aligned} \tag{1}$$

$$\begin{aligned}
 DOP &= \sqrt{S_1^2 + S_2^2 + S_3^2} / \sqrt{S_0^2} \\
 DOLP &= \sqrt{S_1^2 + S_2^2} / \sqrt{S_0^2} \\
 DOCP &= \sqrt{S_3^2} / \sqrt{S_0^2}
 \end{aligned} \tag{2}$$

### 3. RESULTS

#### 3.1 Lipid emulsion concentrations

High-resolution spectrometer (Ocean Optics, Dunedin, FL, USA) measurements in Figure 2 show that the reflectance spectra of our lab-made LE phantoms closely followed the published Intralipid trends [17-19], thereby validating their ability to replicate the scattering characteristics of commercial Intralipid. We note that as the LE concentration increased, the reflectance also increased due to increased backscattering and reduced photon penetration, as shown in Figure 3. Reflectance values above one for 1.25% – 10% LE arise from differences in surface scattering properties between the phantom surface and white calibration tile used to normalize reflectance values. While the reference tile exhibits diffuse reflection, the phantom surface is smooth and moist, leading to enhanced specular reflection and increased collection of reflected light by the imaging probe.

Imaging the phantoms with our handheld probe illustrated a positive correlation between reflectance and concentration, as shown in Figure 3. Regarding polarization sensitivity, Figure 4 showcases that from concentrations of LE from 0.625% – 10%, the polarization difference is relatively small. We concluded that for the phantom to yield the desired DOP values while mimicking the high scattering of biological tissue, we would need to make a lower concentration LE, specifically one prepared at 1% and diluted to a final concentration of 0.1%, allowing for high polarization sensitivity.

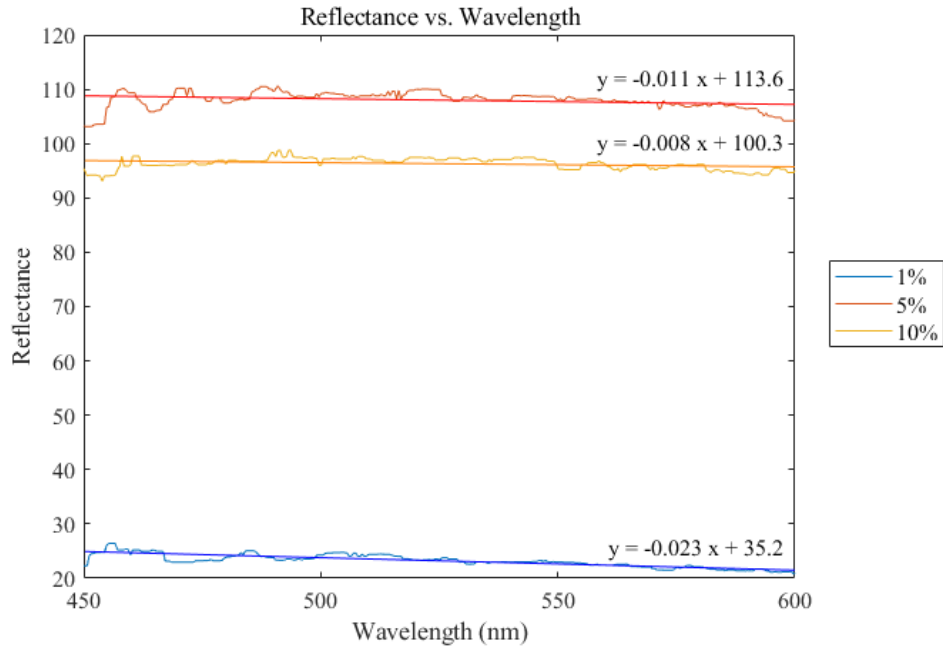


**Figure 2.** Validation of 1%, 5%, and 10% samples using the spectrometer. All samples show that the reflectance of the LE decreases with increasing wavelength over the visible range. However, the 1% sample has a more pronounced decrease than the 5% and 10% samples. The latter have flatter spectra, demonstrated by the smaller magnitude of the slope of their best fit line.

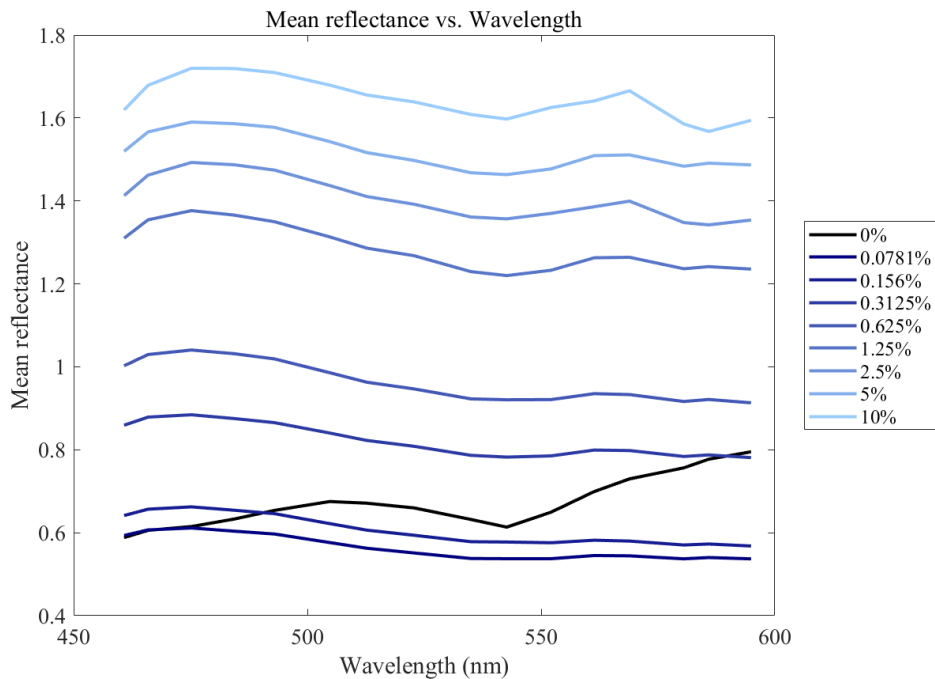


**Figure 3.** Reflectance measurements of LE phantoms. As the concentration of LE increases, the mean reflectance values also increase due to additional multiple scattering events. The shape of the LE phantom spectra differs from that of the 0% control, which contains DI water instead of LE. This sample therefore exhibits reduced absorption and scattering, resulting in increased photon penetration depth and greater contribution from bottom surface back-reflection.

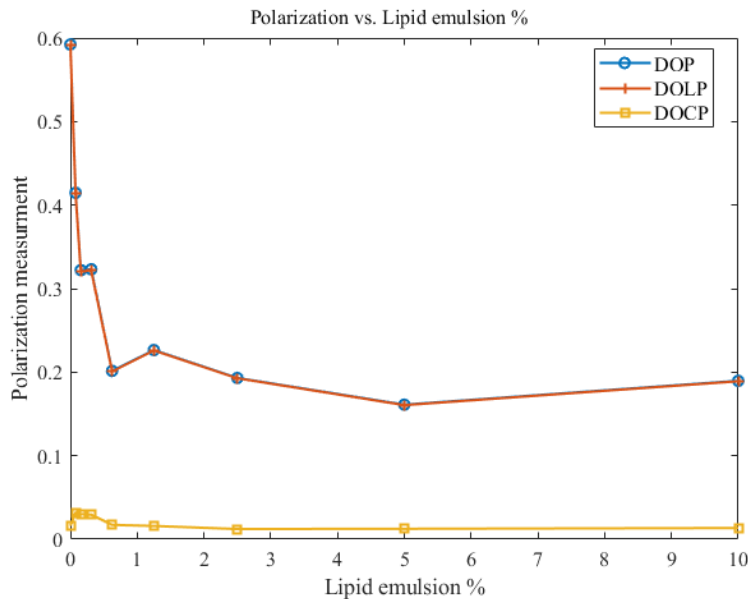


**Figure 4.** Polarization measurements across LE phantoms of different concentrations. The difference in polarization measurements is much greater at LE concentrations below 0.625%. Above that, the polarization spectra are relatively flat, indicating low polarization sensitivity. Due to the low DOCP values, DOP and DOLP curves almost overlap.

### 3.2 Absorbing medium results

Figure 5 shows that when comparing the effect of blue FC and TS pigments to MB dye in the LE phantom at equal concentrations, the FC led to a decrease in DOP, even lower than that of the LE phantom without any other medium added. The LE phantom without additional dyes or pigments corresponds to the “zero-concentration” condition for all three tested substances. The decrease in DOP when using FC and TS results from the tendency of pigments to have a larger particle size, subsequently increasing scattering and lowering the DOP. In addition, as the concentration of the pigments increased, they tended to show similar or even slightly lower DOP compared to the LE alone. Based on these results, we concluded that we would incorporate dyes instead of pigments into the LE phantoms to control for additional scattering agents like pigments and better observe the absorptive effect of dyes. This test also demonstrated how the PHSI system could distinguish between the variations in both the type and concentration of LE and absorbing mediums.

### 3.3 Concentration of dye in phantoms

During preliminary testing of each dye concentration, stock solution concentrations were selected by systematically titrating dye concentrations and examining the relationship between changes in absorption and polarization as a function of wavelength. If too much dye was added, the reflectance values would be too low due to high absorption, which could potentially lead to inaccurate calculation of polarization properties. On the other hand, if very little dye was added, the color of the stock solution would appear too light, and the solution's scattering properties of the LE would overpower the absorbing properties of the dye. This would cause the polarization trends of the dye phantom to resemble that of the LE control phantom instead of the specific dye we were trying to analyze. Therefore, after experimenting with multiple concentrations of each dye and adjusting according to measured polarization values, we determined an ideal set of concentrations for four different dyes that proved a consistent correlation between polarization and absorbance trends. Figure 6 shows the result of systematic testing of various concentrations of each dye. We determined that 0.2% safranin, 0.002% tartrazine, 0.2% crystal violet, and 0.00025% methylene blue were the concentrations that, when added to the LE phantoms, resulted in reflectance and polarization spectra most consistent with absorption modifying photon path length in a scattering medium.

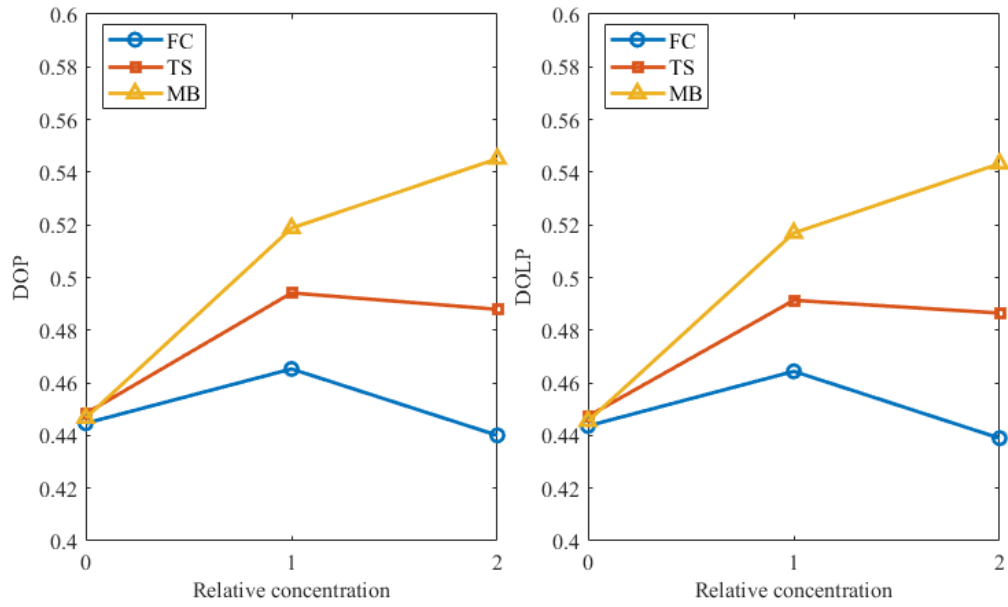


**Figure 5.** Polarization measurements of LE phantoms with blue absorbing mediums at different concentrations. The left plot shows DOP, and the right plot shows DOLP.

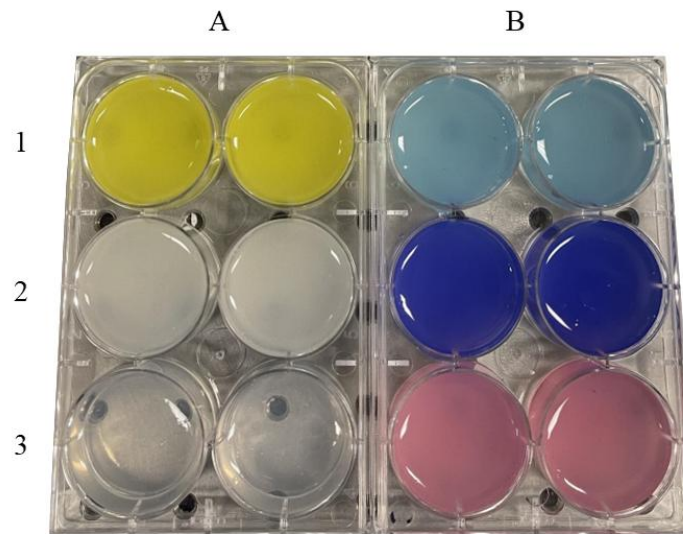


**Figure 6.** LE-dye phantoms in well plates. A1: tartrazine, A2: LE only, A3: DI water only, B1: methylene blue, B2: crystal violet, and B3: safranin.

### 3.4 Validation results

Imaging the phantoms with our PHSI probe showed that across most dyes, DOP peaked near each dye's absorption maximum, demonstrating that selective absorption reduces multiple scattering and thus depolarization of detected photons. The presence of absorbing dyes in the LE-dye phantoms leads to an increase in detected polarization because the dyes reduce the fraction of depolarized (highly scattered) light rather than polarizing light directly. Figure 7 shows that the LE phantom with tartrazine has a DOP peak of 0.75 at ~460 nm, while with safranin it peaked at 0.56 near 513 nm. LE

phantom with crystal violet exhibited elevated DOP beyond 540 nm. For the LE with methylene blue, the DOP spectrum remained relatively flat. Although methylene blue does not absorb strongly in this range and its absorption maximum lies beyond our camera's wavelength, the lack of pronounced increase in DOP toward the longer wavelengths could be due to insufficient methylene blue concentration. This results in the wavelength dependence of the LE working against the dye-dependent wavelength dependence of polarization.

Although the incident light was linearly polarized, the reflected light exhibited a small but non-zero DOCP due to multiple scattering within the lipid emulsion. Successive Mie scattering events introduce differential phase shifts between orthogonal electric field components, generating weak circular polarization that persists in the backscattered signal [20].

In addition to detecting spectral differences, the HSI-synthetic RGB images show that our probe has high resolution and is sensitive enough to detect minute surface textures in the phantoms even though they visually appear to be flat and smooth. The surface exhibits different optical boundary conditions depending on the curing interface. Surfaces cured against the plastic well plate were smoother and had fewer air bubbles, whereas air-exposed surfaces appeared rougher. Measurements were therefore acquired consistently from the side of the phantom cured against the plastic surface.

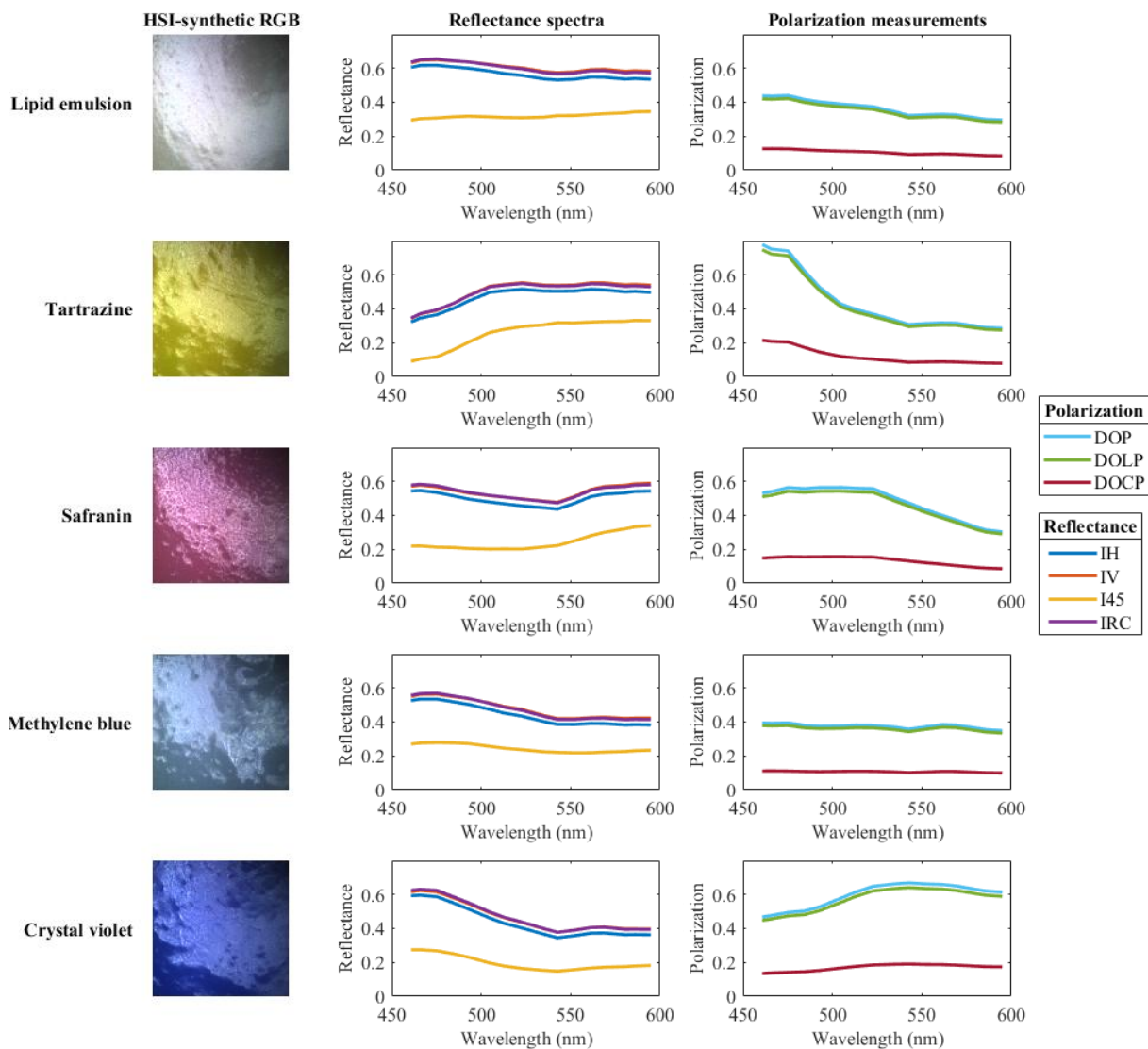


**Figure 7.** Reflectance and polarization measurements of LE phantoms with different dyes. Left panel: HSI-synthetic RGB image, Middle panel: reflectance measurements, and Right panel: polarization measurements for each sample.

### 3.5 External factor testing and observations

Regarding physical stability, it was observed that compared to freshly made phantoms, phantoms stored for two weeks or longer in a 4°C refrigerator shrunk by 2 cm. Figure 8 shows that the phantom color also appeared lighter and more muted over time. Additionally, as the phantoms were constantly handled and imaged, the structural integrity of the phantoms gradually deteriorated because they have a firm hydrogel-like consistency rather than a fully solid form. Chipping on the sides was a common occurrence due to removing the phantoms from their wells and placing them back before and after imaging. Air bubbles were minimized to the best of our ability while creating the phantom; however, some phantoms had inconsistencies due to the byproduct of pipetting and manual mixing with a stirring rod. Future work aims to improve the integrity of the phantoms to maintain consistent imaging and optical stability over time.

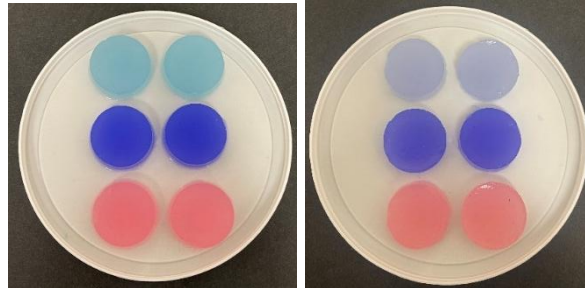


**Figure 8.** Color change of the phantoms from fresh (L) to two weeks later (R).

Due to the optically translucent property of the phantom and the sensitivity of the imaging probe, we observed that the texture and color of the surface underneath the phantom influenced polarization and reflectance measurements. In Figure 9, the top row shows that for a LE phantom imaged on top of a white surface, the white imaging board introduces an additional retro-scattering layer that returns photons back toward the detector. This secondary reflection increases the apparent reflectance of the phantom, particularly at lower scattering concentrations. It also increases the number of scattering events by including photons which pass through the gel twice and are scattered in the background, resulting in a lower DOP in the detected light. In contrast, a black background absorbs photons on the ‘bottom’ boundary and minimizes back-reflection, leading to a lower total detected intensity but better selection of changes in light polarization due to the gel, as shown in the bottom row in Figure 9. We also note that while the DOP magnitude differs between the black and white boundary conditions, the shape of the curves are similar.

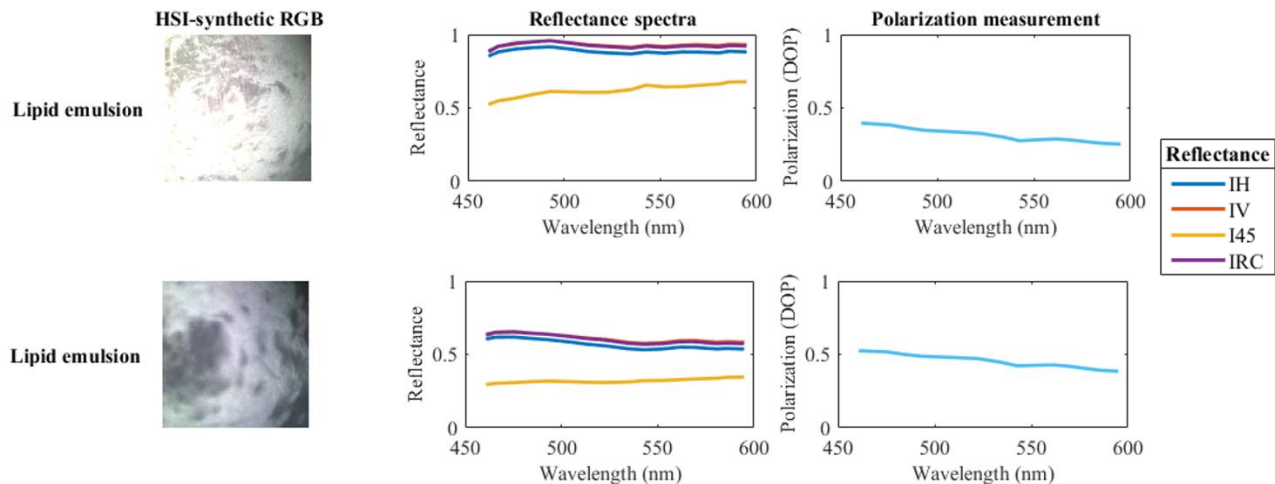


**Figure 9.** LE phantom imaged on a white surface (top row) and black surface (bottom row). The reflectance values are higher and DOP lower when imaged on a white surface compared to a black one.

## 4. DISCUSSION AND CONCLUSION

Our tissue-mimicking LE-dye phantoms offer a fresh, accessible, easy-to-prepare, and tunable method to validate polarized hyperspectral imaging systems. Unlike some commercial alternatives, they require no prescription or long-term storage and can be customized in volume and concentration for cost-effective scattering analysis. They simulate chromophore absorption and tissue-like scattering properties across broadband wavelengths, providing a sufficient foundation for robust system evaluation and serve as a practical tool for developing clinical imaging probes and optimizing system performance. Our results show that for most of the dyes tested, there was elevated DOP and reflectance dip near each dye's absorption maximum. This indicates that selective absorption reduces multiple scattering and depolarization. In addition to being able to detect spectral differences in reflectance and DOP, our probe's high resolution and sensitivity further demonstrate that the probe can resolve differences in surface textures despite the phantom appearing smooth.

For future iterations of this work, we will validate the scattering properties of our lab-made LE to commercial Intralipid using both the spectrometer and our handheld probe as well as measure other optical parameters such as absorption and reduced scattering coefficients. These will be valuable in determining ways to minimize and or standardize boundary conditions. We will also test a wider range of dyes that have more distinct absorbance features within the 460 – 600 nm range, such as trypan blue and rhodamine B. Finally, we will improve the long-term stability of the phantoms to minimize degradation over time.

## ACKNOWLEDGEMENTS

Research reported in this publication was supported in part by the National Cancer Institute of the National Institutes of Health under Award Number R01CA288379 and by the Cancer Prevention and Research Institute of Texas (CPRIT) under Award Number RP240289 and RP240542. The content is solely the responsibility of the authors and does not necessarily represent the official views of the National Institutes of Health.

## REFERENCES

- [1] P. Ghassemi, T. E. Travis, L. T. Moffatt, J. W. Shupp, and J. C. Ramella-Roman, "A polarized multispectral imaging system for quantitative assessment of hypertrophic scars," *Biomed Opt Express*, 5(10), 3337-54 (2014).
- [2] F. Vasefi, N. MacKinnon, R. B. Saager, A. J. Durkin, R. Chave, E. H. Lindsley, and D. L. Farkas, "Polarization-sensitive hyperspectral imaging in vivo: a multimode dermoscope for skin analysis," *Sci Rep*, 4, 4924 (2014).
- [3] L. Ma, A. Srinivas, A. Krishnamurthy, X. Zhou, N. S. Shah, G. Obaid, and B. Fei, "Automated Polarized Hyperspectral Imaging (PHSI) for ex-vivo and in-vivo Tissue Assessment," *Proc. SPIE* 12391, 123910F (2024).
- [4] H. K. Mubarak, X. Zhou, D. Palsgrove, B. D. Sumer, A. Y. Chen, and B. Fei, "An ensemble learning method for detection of head and neck squamous cell carcinoma using polarized hyperspectral microscopic imaging," *Proc. SPIE* 12933, 129330P (2024).
- [5] X. Zhou, L. Ma, H. K. Mubarak, D. Palsgrove, B. D. Sumer, A. Y. Chen, and B. Fei, "Polarized hyperspectral microscopic imaging system for enhancing the visualization of collagen fibers and head and neck squamous cell carcinoma," *J Biomed Opt*, 29(1), (2024).
- [6] X. Zhou, H. K. Mubarak, L. Ma, D. Palsgrove, B. D. Sumer, and B. Fei, "Polarized hyperspectral microscopic imaging for collagen visualization on pathologic slides of head and neck squamous cell carcinoma," *Proc. SPIE* 12382, 1238204 (2023).
- [7] X. Zhou, H. K. Mubarak, L. Ma, D. Palsgrove, S. Ortega, G. M. Callico, E. A. Medina, B. B. Brimhall, M. Whitted, and B. Fei, "Polarized hyperspectral microscopic imaging for white blood cells on Wright-stained blood smear slides," *Proc. SPIE* 12382, 1238207 (2023).
- [8] J. C. Sherey, L. Ma, A. M. Ha, C. Lane, and B. Fei, "Validation of a handheld polarized hyperspectral imaging probe on intralipid phantom and mouse tissue," *Proc. SPIE* 13322, 1332204 (2025).
- [9] G. Chapman, I. Aguilera, and M. Schilling, "Fast scattering coefficient measurement of intralipid-infused tissue phantoms using imaging sensors," *Proc. SPIE* 12840, 1284002 (2024).
- [10] P. Lai, X. Xu, and L. V. Wang, "Dependence of optical scattering from Intralipid in gelatin-gel based tissue-mimicking phantoms on mixing temperature and time," *J Biomed Opt*, 19(3), 35002 (2014).

- [11] L. Hacker, H. Wabnitz, A. Pifferi, T. J. Pfefer, B. W. Pogue, and S. E. Bohndiek, “Criteria for the design of tissue-mimicking phantoms for the standardization of biophotonic instrumentation,” *Nat Biomed Eng.*, 6(5), 541–558 (2022).
- [12] L. Cortese, G. L. Presti, M. Pagliazzi, D. Contini, A. D. Mora, A. Pifferi, A. Konugolu Venkata Sekar, L. Spinelli, P. Taroni, M. Zanoletti, U. M. Weigel, S. de Fraguier, A. Nguyen-Dihn, B. Rosinski, and T Durduran, , “Liquid phantoms for near-infrared and diffuse correlation spectroscopies with tunable optical and dynamic properties,” *Biomedical Optics Express*, 9(5), 2068-2080 (2018).
- [13] M. Kim, S. Im, I. Park, D. Kim, E. S. Kim, J. Joseph, and J. Yoon, “Fabrication of agar-based tissue-mimicking phantom for the technical evaluation of biomedical optical imaging systems,” *Current Applied Physics*, 61, 80-85 (2024).
- [14] M. Lepore and I. Delfino, “Intralipid-Based Phantoms for the Development of New Optical Diagnostic Techniques,” *The Open Biotechnology Journal*, 13, 163-172 (2019).
- [15] P. Di Ninni, Y. Bérubé-Lauzière, L. Mercatelli, E. Sani, and F. Martelli, “Fat emulsions as diffusive reference standards for tissue simulating phantoms?,” *Applied Optics*, 51(30), 7176-7182 (2012).
- [16] D. J. McClements, [Food emulsions: principles, practices, and techniques] CRC press, (2004).
- [17] M. D. Singh and I. A. Vitkin, “Discriminating turbid media by scatterer size and scattering coefficient using backscattered linearly and circularly polarized light,” *Biomed Opt Express*, 12(11), 6831-6843 (2021).
- [18] S. C. Kanick, V. Krishnaswamy, U. A. Gamm, H. J. C. M. Sterenborg, D. J. Robinson, A. Amelink, and B. W. Pogue, “Scattering phase function spectrum makes reflectance spectrum measured from Intralipid phantoms and tissue sensitive to the device detection geometry,” *Biomed Opt Express*, 3(5), 1086-100 (2012).
- [19] S. T. Flock, S. L. Jacques, B. C. Wilson, W. M. Star, and M. J. van Gemert, “Optical properties of Intralipid: a phantom medium for light propagation studies,” *Lasers Surg Med*, 12(5), 510-9 (1992).
- [20] H. J. van Staveren, C. J. M. Moes, J. van Marie, S. A. Prahl, and M. J. C. van Gemert, “Light scattering in Intralipid-10% in the wavelength range of 400-1100 nm,” *Appl Opt*, 30(31), 4507-14 (1991).